THEORETICAL SIMULATION AND EXPERIMENTAL VALIDATION OF A CLOSED LOOP NATURAL CIRCULATION COOLING SYSTEM FOR A TANK CONTAINING INTERNALLY HEAT GENERATING MATERIAL

Du Toit, IS and Dobson, RT

Department of Mechanical and Mechatronic Engineering, University of Stellenbosch,
Stellenbosch, Private Bag XI, MATIELAND, 7602, South Africa
Tel 27 (0)21 8084286, fax 27 (0)21 8084958, e-mail, rtd@sun.ac.za, coenraad@sun.ac.za

Abstract

This paper relates to the cooling of a tank containing a toxic material in which heat is being internally generated. Such tanks are extensively used in chemical reaction tanks in which exothermic reactions are taking place, and in the nuclear industry, for the storage of so-called high-level radioactive waste such as spent fuel. Many of these tanks use forced convection for their cooling. The object of this paper is to present a closed loop natural circulation cooling system for such an internally heat-generated tank in which no external power is required and in which any leakage of toxic material to the environment is prevented by it being totally contained in a steel lined structure, and in which no forced or natural convection air leakage paths exist. The design will be presented, discussed and explained. The assumptions needed for the derivation of the difference equations constituting the theoretically simulation model will be given, and the theoretical model solved using a computer program. A small laboratory-scale model of such a system has been built and experimentally tested and evaluated, under start-up transient, dynamic and steady-state conditions as well as for single and two-phase operating modes. The experimental results are compared with the theoretically generated results and their validity discussed, conclusions are drawn and it is suggested that the theoretical model captures remarkably-well much of the physical behavioural characteristics of the natural circulation cooling system.

Keywords: Natural circulation, cooling, closed-loop thermosyphon, heat exchanger, two-phase flow and heat transfer

1 Introduction

This paper relates to the Pebble Bed Modular New Technology Development program and in particular to the cooling of the spent/used fuel storage tanks, with a natural circulation passive cooling system. The PBMR is a Generation IV graphite moderated, high temperature, gas cooled reactor recently developed in South Africa. It will make use of spherical fuel and continuous fuelling technology (Fuls and Mathews, 2006). PBMR fuel spheres are recycled through the reactor up to six times before they are regarded as *spent* fuel. Interim and final storage are thus required. Because the radioactivity decays over a long time, provision must be made to remove the heat generated in the storage tanks, especially in the case of fuel spheres that are stored temporarily in the storage tanks, prior to being recycled through the reactor again.

In figure 1 a concept for a passive cooling system is shown. The fuel storage tank is surrounded by a jacketed cooling sleeve which forms the primary evaporator. The cooling jacket around the fuel storage tank is connected to a piping system that forms the primary natural circulation loop. As the temperature of the fuel storage tank increases the density of the primary coolant (water) decreases, and this causes a density difference between the riser section and liquid return section. The density difference in turn will cause a resulting pressure difference between the riser and liquid return section resulting in coolant flow, in the primary loop. The heat removed from the fuel storage tank is transferred from the primary loop to the secondary loop via the primary heat exchanger. The physical barrier between the primary condenser and secondary evaporator is to ensure that no radioactive waste is transferred from the primary loop, which is situated within the containment building, to the secondary heat transfer loop; the secondary loop will be in direct contact with the

environment. The secondary heat transfer loop will also be in the form of a closed loop thermosyphon type a heat pipe, with the secondary condenser being an air-cooled heat exchanger that will be cooled by natural draft. Note that the proposed system is termed an entirely passive cooling system and that there will be no mechanical moving parts, such as pumps or electronic operated valves and controls; thereby significantly improving the safety and reliability.
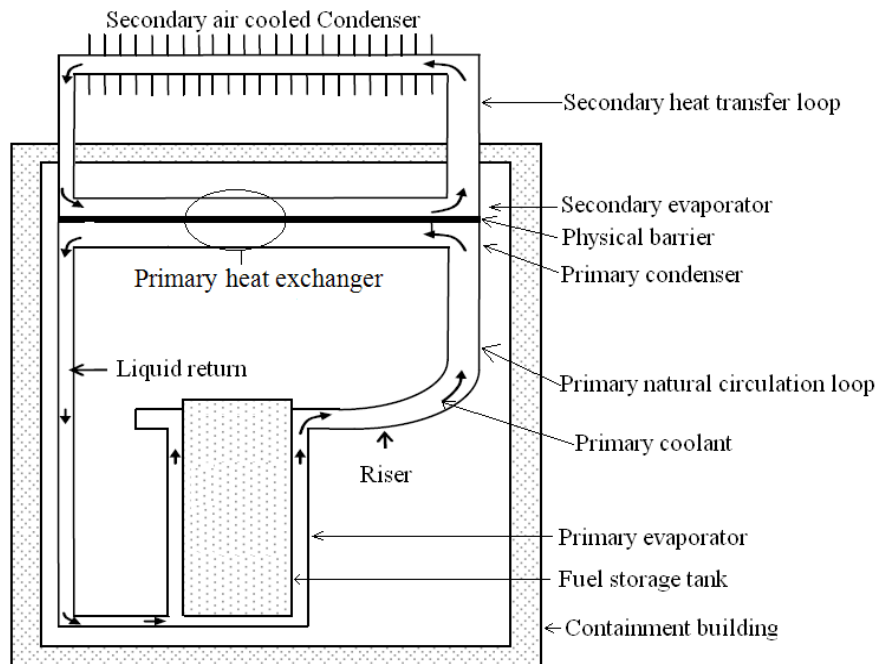

Figure 1 Passive cooling concept for spent nuclear fuel storage (Dobson, 2010)

The spent/used fuel has to be stored for a period of up to 80 years; this includes the 40 years expected operation life time of the PBMR plant and an additional 40 years on site storage after discontinuing the plant. Thus the storage tanks must have a minimum lifetime of 80 years (Viljoen et al., 2005). Given the long life time of the storage tank they must be protected from corrosion for the entire lifetime to ensure their integrity. The storage tanks are pressure vessels and thus the material used for their construction is limited by the ASME boiler and pressure vessel code to a carbon steel and temperature not exceeding 250 ˚C. Thus stainless steel is not a feasible option, given the tendency for forming stress corrosion cracking in a chlorine environment.

The importance of the more extensive use of natural circulation loops in cooling systems is highlighted in IAEA, Techdoc-1474 (2005) and may be summarised as follows:
According to IAEA-TECDOC-1474, the wide use of natural circulation loops in the cooling of the residual heat from nuclear reactors is chosen for the following advantages, above forced convection cooling.
- Simplicity is the overwhelming contributor to the safety of a natural circulation loop, the removal of active power from the cooling system greatly reduces the risk of losing coolant to remove residual heat from the reactor. The use of natural circulation simplifies the construction, maintenance and operation of the system. The elimination of coolant pumps greatly reduces accident scenarios associated with loss of coolant.
- The flow characteristic as a function of power greatly increases in two-phase operation for natural circulation system, this means that the mass flow rate of the coolant in the loop increases as a function of the residual heat whereas the mass flow rate in a forced convection system increases as a function of added mechanical power.
- Low pumping head of natural circulation systems, entails that large reservoirs are needed to keep the power density of the cooling fluid low, this makes the cooling system thermal response slow and increases the time that operators have to react to various upsets in the system.

Described above are some of the advantages of natural circulation system. Natural circulation systems are not without disadvantages and these are given by IAEA-TECDOC-1474 as:

- The mass flow rate is a function of the power removed from the systems so to increase the mass flow rate at a constant heat input, the height difference between the heat sources and sink must be increase, which leads to increase in capital cost.
- A general natural circulation loop starts off from single phase flow and progresses to two-phase flow as the heat removed increases. This can cause stability problems and may lead to oscillation in the cooling fluid, this phenomenon is highly dependent of geometry and will differ from system to system.

The work presented in this paper is based on a mechanical engineering project (du Toit, 2010) and the specific objectives of this paper are:

- Undertake a literature survey on the current available techniques of cooling spent/used nuclear fuel.
- Design and build an experimental setup of the proposed Double-Vapour chamber isolated heat exchanger setup, excluding the secondary loop with the air-cooled heat exchanger. Replace the air-cooled heat exchanger with a continuous cooling water system, in such a manner that a continuation of the project can add the secondary heat transfer loop onto the existing experimental setup.
- Obtain experimental results and with these determine the heat transfer coefficients of the primary evaporator and the primary condenser.
- Write a computer program that simulates the transient behaviour of the system, with the experimentally calculated heat transfer coefficients.

Leading from this Introduction and these objectives the experimental set-up that was built and tested is given in section 2. In section 3 the theoretical simulation model for the flow and heat transfer in the loop is presented. In section 4 the experimental and theoretical simulation results are given, and finally in section 5 the finding are discussed, conclusions drawn and recommendations made.

2 Experimental set-up

The experimental set-up is shown schematically in figure 2, where the dashed lines indicate the connection of the different measuring components to the data logger, while figure 3 is an annotated photograph of the equipment in the laboratory. A sectional view through the heating jacket is given in figure 4 and a photgrapgh of the heating element is given in figure 5.

Of particular interest is the primary heat exchanger (details of which are shown in figures 6, 7 and 8). As shown in figure 7 the primary heat exchanger consists of a primary condenser and a secondary evaporator separated by a thermally conducting physical barrier. The barrier must be able to allow heat to be transferred but must act as an absolute barrier for diffusion of any radioactive isotopes, for example tritium H^3. In this design any non-condensible gas that may be liberated from the coolant must be able to move freely under the influence of gravity to the highes point in the loop, where it can be safely and readily removed. Counter-wise, any droplet of lquid coolant in the loop must also be able to move freely under the influence of gravity to the lowest point where provision must be made to be able to drain the liquid from the system.

Figure 2 Experimental equipment layout

Figure 5 Two 3 kW heating elements
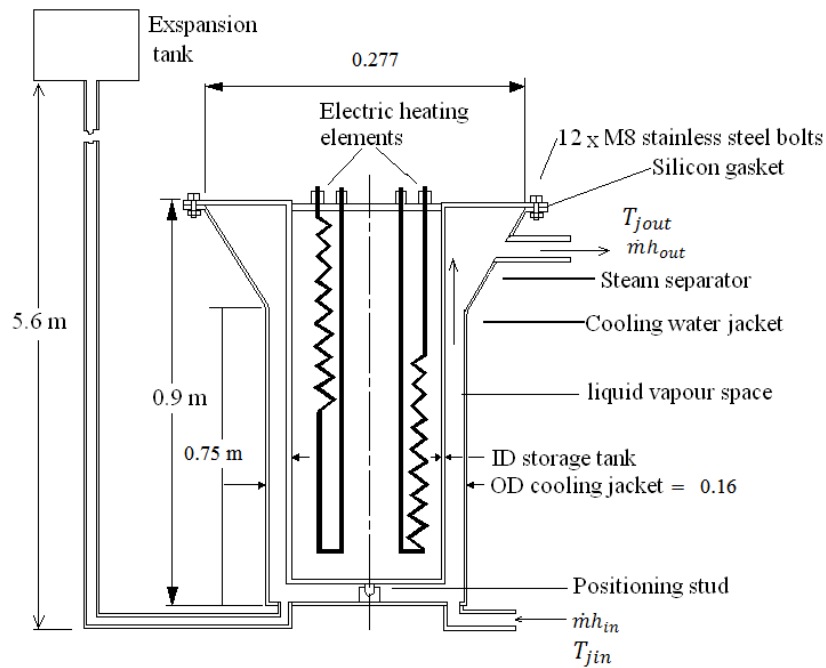
Figure 3 Experimental equipment layout

Figure 4 Section of the jacketed heating tank with electrical heating elements simulating the heat source
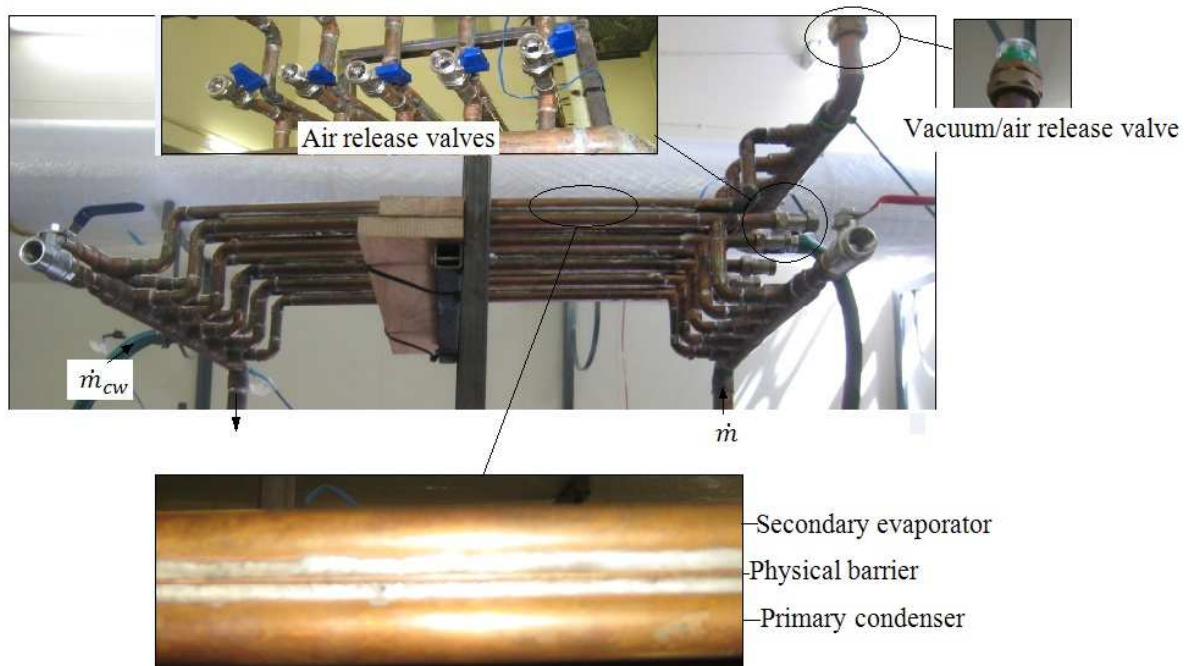

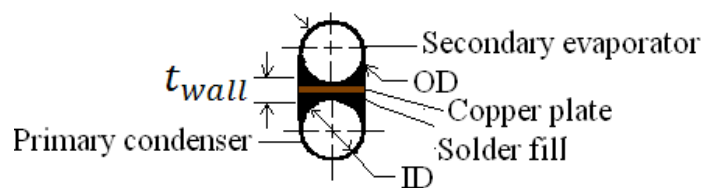Figure 6 Photograph of primary heat exchanger

Figure 8 Cross sectional view of a single pipe of the primary heat exchanger, showing solder detail.
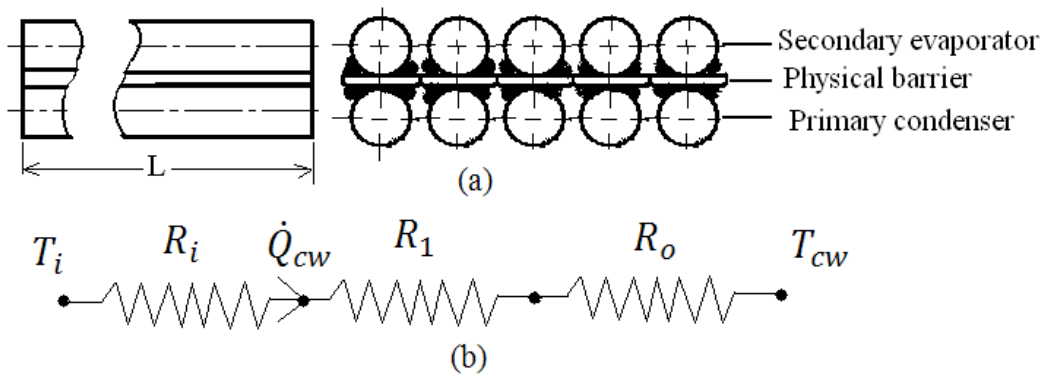
Figure 7 Primary heat exchanger design layout, (a) Primary heat exchanger, (b) thermal resistance diagram between primary condenser and secondary evaporator

3 Theory

There are a number of assumptions that are made in developing the mathematical simulation model: quasi-static equilibrium, incompressible flow and one-dimensional flow. Each of the assumptions will be discussed below.

When a process proceeds in such a manner that the system remains infinitesimally close to equilibrium state at all times, it is called a quasi-static process (Cengle and Boles, 2007). This is a valid approximation seeing that the maximum velocity of the water as working fluid in the primary loop will be at least 3 orders of magnitude less than the speed of sound in the working fluid. This means that the rate at which the pressure waves propagate throughout the system is orders higher than the rate at which the mass flow and heat transfer takes place in the loop. By using this approximation it is justifiable to do a steady state analysis at each time step and in doing so, a transient behaviour of the system can be obtained if the time steps used are small enough.

Flow can be assumed to be incompressible if the Mach number is less than 0.3, where V is the particle velocity of the fluid and c is the speed of sound in the fluid (± 2000 m/s for water). The speed of sound in water vapour will vary as function of temperature and can be calculated by $c = \sqrt{kRT}$ with k being the specific heat ration, R being the gas constant and T being temperature in Kelvin (Cengel and Cimbala, 2006). The buoyancy force that will drive the flow, changes according to temperature, thus meaning that it is not feasible to incorporate constant density flow. If however the Boussinesq approximation is adopted then it can be assumed that the density stays constant accept where it is multiplied by the g, the gravitational acceleration (CENGEL, Y.A, 2006). This is however not a valid approximation when two-phase flow is considered and thus for the mathematical model the momentum flux term will be left in and used in the computer code for the conservation of momentum. The Boussinesq approximation can however be used with confidence in single phase buoyancy driven flow. A one-dimensional solution will be, because a two dimensional solution, for two-phase flow is to complex.

In figure 9 the passive cooling system is divided into discrete control volumes. The bottom pipe that contains the orifice plate is labelled N1, this section is divided into 2 control volumes. The primary evaporator is divided into 6 control volumes and is labelled N2a, the vertical pipe connecting the primary evaporator to the primary condenser is divided into 2 control volumes and is labelled N2b. The combination of N2a and N2b is N2 which represents the left hand side vertical section of the loop. The primary condenser and secondary evaporator is divided into 5 control volumes, this section is labelled N3. The vertical pipe connecting the primary evaporator to the bottom pipe is divided into three control volume and is labelled N4. The pipe connecting the primary loop to the expansion tank is divided into 2 control volumes and is labelled N5a and the expansion tank is divided into 2 control volumes and labelled N5, the combination of N5a and N5b to gives N5.
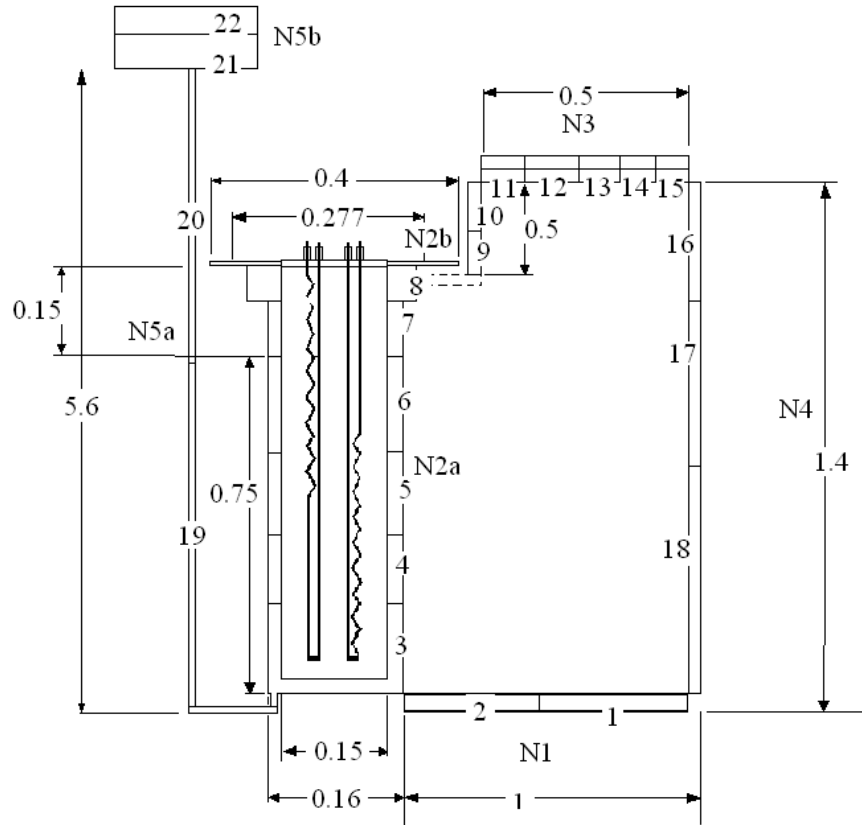
Figure 9 Control volume discretisation of the primary coolang natural circulation cooling system

3.1 Conservation of energy

The equation of motion may be written as (White, 2005)

$$\frac{d}{dt}(E_{sys}) = \frac{dQ}{dt} - \frac{dW}{dt} = \frac{d(em)}{dt} + e\rho v A_{out} - e\rho v A_{in} \qquad (5.8)$$

In Equation 5.8 the work term can be ignored seeing that no work is performed in the fluid and boundary work done is ignored. Where $e = u$ for the fluid in the control volume and $e = h$, for the fluid moving across the control volume boundaries. Taking the above into consideration Equation 5.8 reduces to:

$$\frac{d(um)}{dt} = \dot{Q}_{in} - \dot{Q}_{out} + \dot{m}(h_{in} - h_{out}) \qquad (5.9)$$

A difference equation can now be derived from Equation 5.9 using the upwind differencing scheme:

$$\frac{\Delta(um)}{\Delta t} = \frac{mcv\Delta T}{\Delta t} = \dot{Q}_{in} - \dot{Q}_{out} + \dot{m}(h_{in} - h_{out}) \qquad (5.10)$$

An explicit formulation of the conservation of energy can now be derived for a general control volume element in the primary evaporator, from Equation 5.10 as:

$$u_i^{new} = u_i + \frac{\Delta t}{m_i^{new}}\left(\dot{Q}_{in_i} - \dot{Q}_{out_i} + \dot{m}(h_{i-1} - h_i)\right) \qquad (5.11)$$

Where, i refers to the control volume under consideration and $i-1$,to the control volume before, and new refferes to the value at the new time step $t + \Delta t$.

Now the new internal energy can be calculated at each new time step, the temperature and the internal energy are related by the following correlation $u = cvT$. When calculating the temperature around the loop, the saturation status of the different control volumes has to be known, the following logical statement was written to calculate x , the vapour to liquid concentration and also calculate the new temperature.

If $u_i^{new} < u_f$ Then:

$$T_i^{new} = \frac{u_i^{new}}{c_v} \quad and \quad X_i^{new} = 0 \tag{5.12}$$

If $u_i^{new} > u_f$ Then

$$T_i^{new} = T_{sat}^{new} \quad and \quad X_i^{new} = \frac{u_i^{new} - u_f^{new}}{u_f^{new}} \tag{5.13}$$

With:

$$u_f^{new} = c_v T_{sat}^{new} \tag{5.14}$$

The difference equation for the conservation of energy is derived from the differential equation for a control volume in the primary loop. From Equations 5.11 to 5.14 the new temperature at time step $t + \Delta t$ can be determined around the loop and the new vapour to liquid content, x of the control volume can be calculated.

This can be applied all around the loop. For the piping section the heat transferred $\dot{Q}_{in_i}$ will be equal to zero. In the primary condenser the heat loss to the environment will be ignored, this term will be replaced by the heat transferred to the secondary evaporator $\dot{Q}_{cw_i}$ as explained in section 4.4, with the experimental heat transfer coefficient.

This section will show how the difference equation was developed for the secondary evaporator.
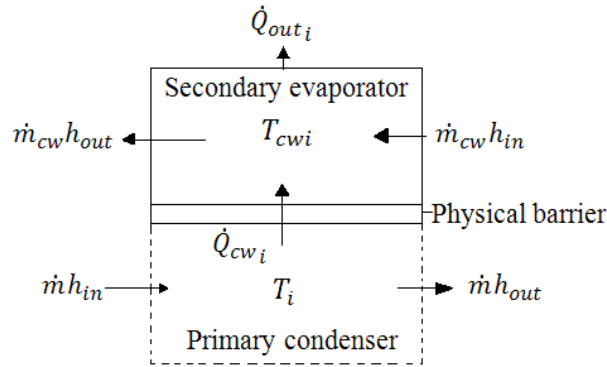

Figure 10 The i'th control volume for the conservation of energy for secondary evaporator.

In figure 10 a typical control volume is shown for the secondary evaporator, the bottom control volume is on the primary evaporator side and the top is the secondary evaporator. The heat flow paths are shown in figure 10. The conservation of energy equations is applied in exactly the same manner as in section 5.3.1 with the results for the difference equation:

$$\Delta u = \frac{\Delta t}{m_{cw_i}^{new}} \left(\dot{Q}_{cw_i} - \dot{Q}_{out_i} + \dot{m}_{cw}(h_{in} - h_{out}) \right) \tag{5.15}$$

From Equation 5.15 and using an explicit formulation with an upwind differencing scheme the difference equation for the conservation of energy in the secondary evaporator becomes:

$$u_{cw_i}^{new} = u_{cw_i} + \frac{\Delta t}{m_{cw_i}^{new}} \left(\dot{Q}_{cw_i} - \dot{Q}_{out_i} + \dot{m}_{cw}(h_{i-1} - h_i) \right) \tag{5.16}$$

Now from Equation 5.16 the new temperatures in the secondary evaporator can be calculated from:

$$T_{cw_i}^{new} = \frac{u_{cw_i}^{new}}{c_v} \tag{5.17}$$

The secondary evaporator will not experience boiling and thus it is not needed to calculate the new vapour content in the control volumes.

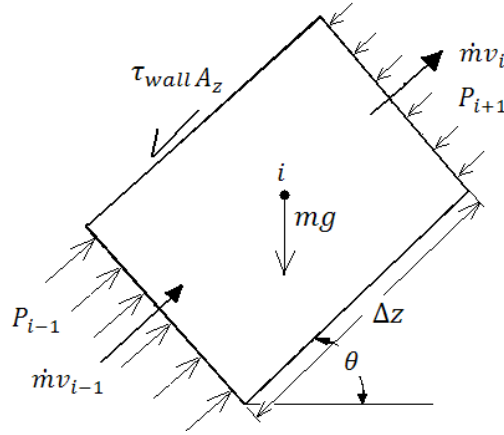## 3.2 Conservation of momentum for a typical control volume

Figure 11 The i th control volume for conservation of momentum

In **Figure 11**figure 11 a general control volume for the conservation of momentum is shown, where; θ is the angle that the control volume lies with respect to the horizontal axis, P is the pressure on the inlet and outlet faces of the control volume, τ_{wall} is the friction loss of the fluid flowing in the control volume and $\dot{m}v$ is the momentum flux moving across the boundary of the control volume.

In Equation 5.6 the differential equation for the conservation of momentum for a control volume is given. By using a one-dimensional solution approaches as explained in section 5.1 the integral reduces to: $\int_{cv} v\rho dV = vm$, by rearranging Equation 5.6 the differential conservation of momentum for a typical control volume becomes:

$$\frac{\partial(mv)}{\partial t} = \Sigma F_z + \dot{m}(v_i - v_{i-1}) \tag{5.18}$$

This is applied to the control volume in Figure 11 with the result being:

$$\frac{\partial(mv)}{\partial t} = \dot{m}(v_{i-1} - v_i) + \left(A_{x_{i-1}}P_{i-1} - A_{x_{i+1}}P_{i+1}\right) - mgSin\theta - \tau_{wall}A_z \tag{5.19}$$

Now the velocity term can be manipulated as follows:

$$v = \frac{\dot{m}}{pA_x} \tag{5.20}$$

And the LHS of Equation 5.19 can be expanded as:

$$\frac{\partial(mv)}{\partial t} = \frac{\partial(m)v}{\partial t} + \frac{\partial(v)m}{\partial t} \tag{5.21}$$

By combining Equations 5.19 to 5.21 the differential equation for the conservation of momentum is expanded to:

$$\frac{\partial(m)v}{\partial t} + \frac{\partial(v)m}{\partial t} = \dot{m}^2\left(\frac{1}{\rho_{i-1}A_{x_{i-1}}} - \frac{1}{\rho_i A_{x_i}}\right) + \left(A_{x_{i-1}}P_{i-1} - A_{x_{i-1}}P_{i+1}\right) - mgSin(\theta) - \tau_w A_z$$

From Equation 5.21 follows:

$$\frac{\partial(v)m}{\partial t} = -\frac{\partial(m)v}{\partial t} + \dot{m}^2\left(\frac{1}{\rho_{i-1}A_{x_{i-1}}} - \frac{1}{\rho_i A_{x_i}}\right) + \left(A_{x_{i-1}}P_{i-1} - A_{x_{i-1}}P_{i+1}\right) - mgSin(\theta) - \tau_w A_z$$

Now by dividing by A_{x_i} and integrating around the loop the differential Equation 5.22 can be reduced to the difference equation.

$$\frac{\Delta v}{\Delta t} = \frac{\frac{\Sigma \dot{m}^2}{Ax_i}\left(\frac{1}{\rho_{i-1}A_{x_{i-1}}} - \frac{1}{\rho_i A_{x_i}}\right) - \Sigma\rho_i\Delta zSin(\theta) - \frac{\Sigma\tau_{wall}A_z}{A_{x_i}}}{\Sigma\rho_i\Delta z} \tag{5.23}$$

Equation 5.23 can now be reduced to a condensed form, that will be easier to implement in the computer program.

$$\frac{\Delta v}{\Delta t} = \frac{A + B - F}{M} \tag{5.24}$$

Where:

$$A = \frac{\sum \dot{m}^2}{A_{x_i}}\left(\frac{1}{\rho_{i-1}A_{x_{i-1}}} - \frac{1}{\rho_i A_{x_i}}\right)$$

$$B = -\sum_i \rho_i \Delta z \mathrm{Sin}(\theta)$$

$$F = \frac{\sum \tau_{wall} A_z}{A_{x_i}}$$

$$M = \sum \rho_i \Delta z$$

Now by using the explicit formulation Equation 5.24 is expanded to:

$$v_i^{new} = v_i + \Delta t\left(\frac{A + B - F}{M}\right) \tag{5.25}$$

Now the new mass flow rate of the primary loop can be calculated from Equation 5.25 as:

$$\dot{m}^{new} = \rho_i A_{x_i} v_i^{new} \tag{5.26}$$

From the above correlation the new mass flow rate for the loop can be determined, at each time step.

4 Results

The experimental and theoretically results (loop mass flow rate and temperatures) are given in figures 12 to 16 as a function of time from start-up for different heating element input powers of I, 2, 3, 4 and 5 kW.. It is seen that the theoretically predicted mass flow rate and temperature response curves capture the experimentally results fairly accurately. As the power increases so to does the mass flow rate increase, thereby illustrating the natural ability of the loop to remove larger poer inputs by naturally increasing the mass flow rate.. For power inputs of up 4 kW boiling did not occur, hoever at an input power of 5 kW the characteristically dynamic and oscillatory flow behaviour is also captured by the theoretical model.
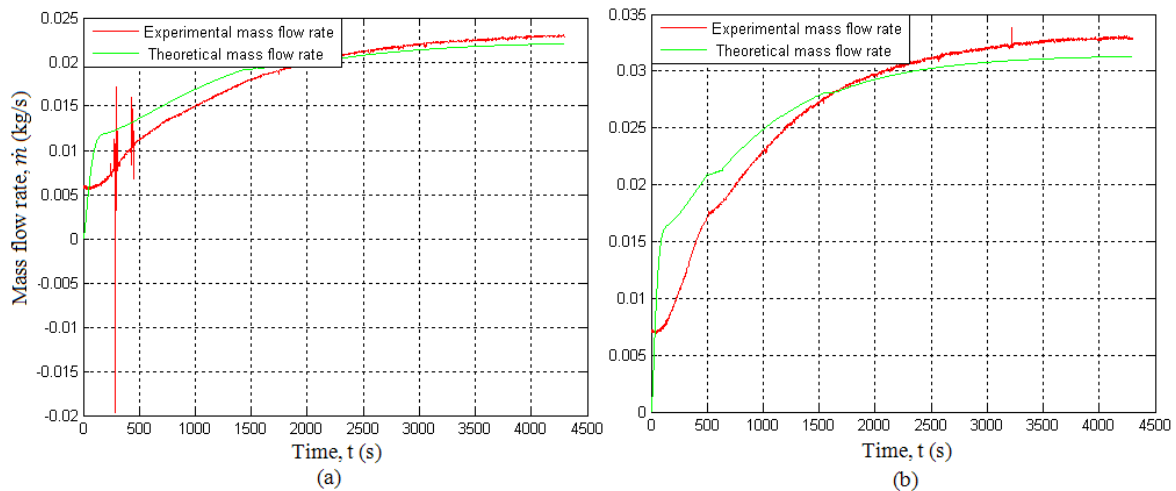

Figure 12 Experimental and theoretical mass flow, (a) for 1 kW power input, (b) for 2 kW input powers

The actual mass flow rate is higher than predicted by the computer program, both for single phase input conditions and two-phase input conditions. For power inputs of 1, 2, 3 and 4 kW the percentage difference at steady state, between the experimental and theoretical mass flow rate is, 4.3 %, 5.45 %, 1.9 % and 4.3 % respectively. Thus the theoretical predicted mass flow rates represent the steady state conditions reasonably well, for single phase steady state operation conditions.
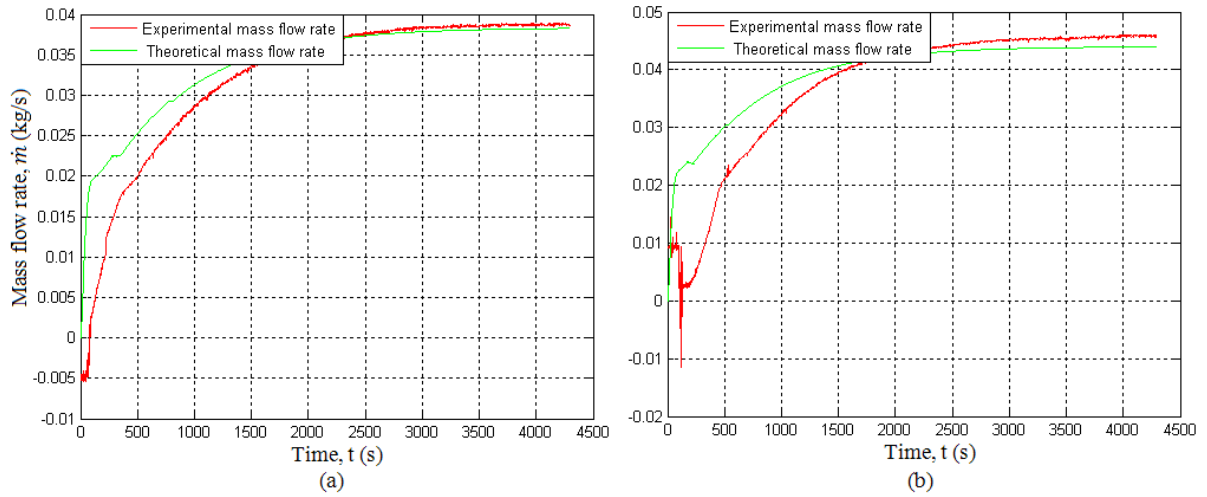
Figure 13 Experimental and theoretical mass flow, (a) for 3 kW power input, (b) for 4 kW input powers
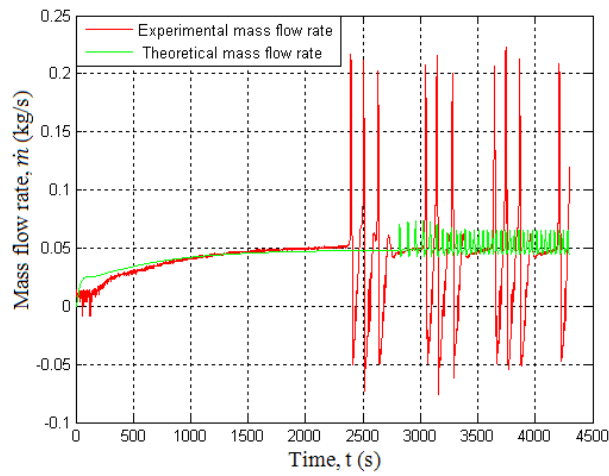

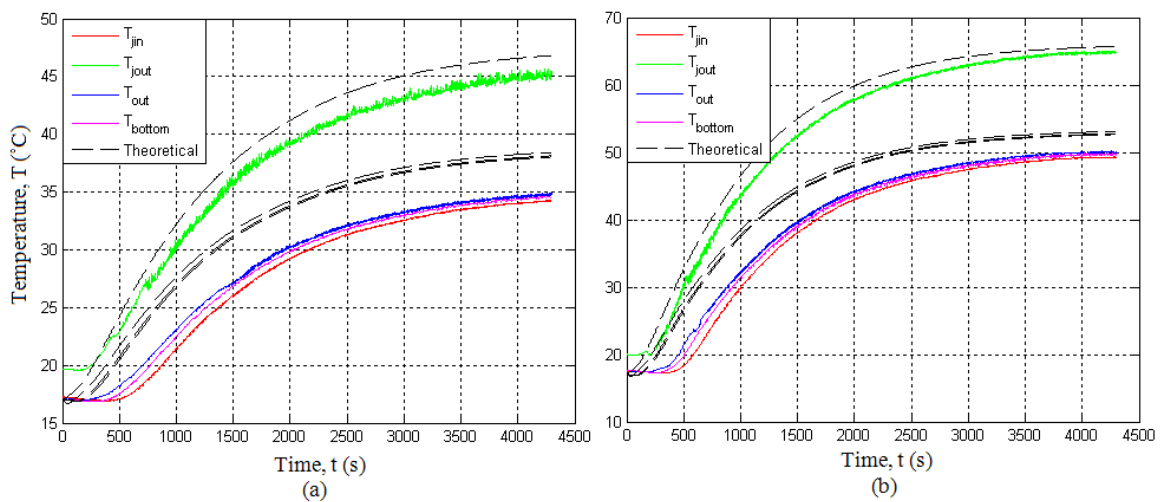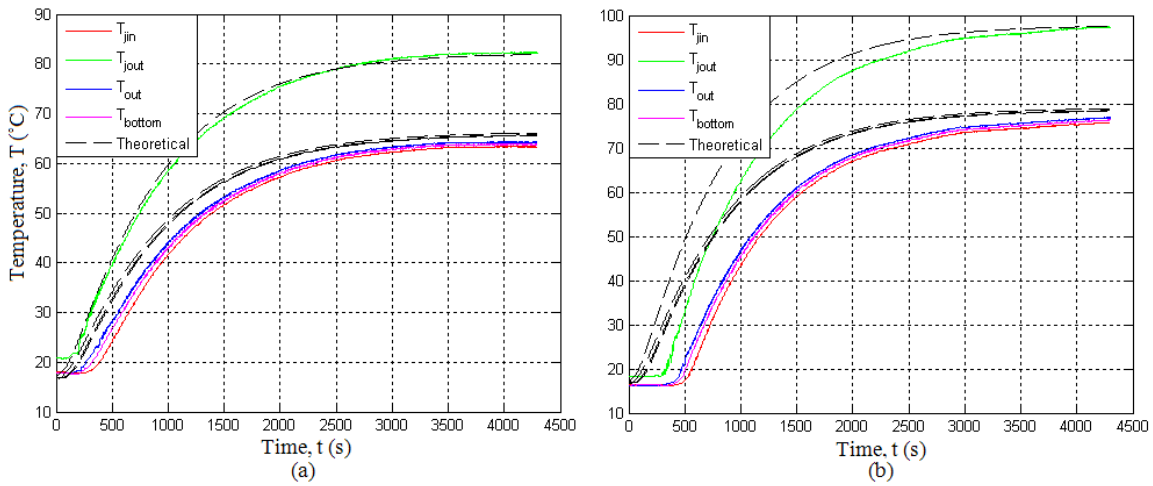Figure 14 Experimental and theoretical mass flow, for 5 kW power input

Figure 15 Experimental and theoretical loop temperatures (a) for 1 kW power input and (b) for 2 kW input powers

Figure 16 Experimental and theoretical loop temperatures (a) for 3 kW power input and (b) for 4 kW input powers
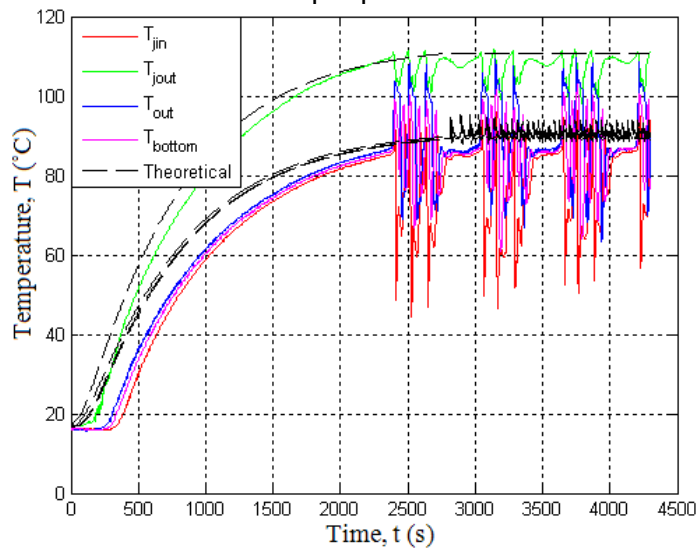

Figure 17 Experimental and theoretical loop temperatures for 5 kW power input

The theoretical predicted temperature distribution around the loop is higher than the experimental temperature distribution. The fluid temperature after the primary evaporator T_{Iout} is reasonably well predicted for power inputs of 1, 2, 3 and 4 kW, the difference between the steady state theoretical predicted values and experimental values is, 4.5%, 2.3 %, 1.5% and 0.5% respectively. As the power input increases the difference between the theoretical and predicted values decreases. The other loop temperatures, $T_{Iin}, T_{out}, T_{bottom}$ are predicted with less accuracy, the differences is in the order of 12 % for 1 kW power input, 6 % for 2 kW power input, 4% for 3 kW power input and 4% for 4 kW power input. The loop temperature is also better predicted for lower power inputs and increases in accuracy with increase in power.

In general for power inputs of 1 kW to 4 KW, the system stabilizes in single phase operation mode. The theory predicts the experimental results reasonably well the mass flow is under predicted, because the theoretical pressure loss coefficients K_L, that was used in the computer code was obtained from general single phase fluid flow from (CENGEL, Y.A and Cimbala, J.M, 2006). It is extremely difficult to predict the pressure loss coefficients. The experimental setup is shown, to accurately predict the pressure loss for such a complex setup is very difficult. The driving force in natural circulation loops is the temperature difference between the heat source and heat sink, the theoretical predicted temperature difference is less than the experimental obtained values. This will also play a part in the under estimation of the experimental mass flow results. Note that the general curve of the experimental data is predicted reasonably well. To improve this, thermal inertia of the system will have to be taken into account; this means that temperature response of the various components of the loop will have to be modelled into the governing equations as done

by(DOBSON, R.T and Ruppersberg, J.C, 2004) in the numerical modelling of a closed loop thermosyphon.

It can be concluded that for input conditions, up to 4 kW, the system stabilizes in a single phase operation conditions, the computer program predicts the transient and steady state values of the system reasonably well. The program underestimates the mass flow rate and over predicts the temperatures in the primary loop.

In figure 14 and 15**Error! Reference source not found.** the mass flow and temperature distribution is shown for a power input of 5 kW, the primary fluid stabilizes in two-phase operation mode. For the experiment setup the primary fluid started to boil at 2400 seconds where the theoretical model predicts that the system starts to boil at 2800 seconds. In Figure the mass flow rate comparison is presented, observed the experimental measured mass flow rate oscillates between 0.2 and -0.05 kg/s, and the theoretical mass flow rate oscillates between 0.043 and 0.07 kg/s. For two-phase flow it is more difficult to estimate the difference between the experimental and theoretical results. However it is quite clear that the computer program does not accurately predict the dynamic behaviour of the mass flow rate of the system once boiling has occurred. The average value is however quite well predicted.

The temperature distribution shown in figure 16, show the same type of results as described for the mass flow rate. However the temperature out of the primary evaporator $T_{i_{out}}$ is predicted to stabilize at the saturation temperature of 110.7 ℃. This is not the case in experimental setup; the temperature of the fluid oscillates around the saturation temperature in the experimental simulation.

The computer program utilises the single phase correlation Equation 4.24 for the calculation of the heat transfer coefficient for the fluid inside the primary condenser. This correlation is only valid for single phase flow and, as seen in figures 14 and 15, this correlation does predict the system response reasonably well, even in two-phase flow.

The computer program utilizes a combined, convection and radiation heat transfer coefficient to determine the heat loss to the environment. This was taken as 5 W/m^{2}K, which is a reasonable assumption. To achieve more accurate results in the prediction of the steady state temperatures of the loop the convection and radiation heat loss must be calculated separately, the convection coefficients will have to be calculated with natural convection correlation as done in Section 4.2, for the energy balance of the system. Currently the computer program does not take this into account, this was done to reduce the complexity of the program; this will be addressed in the recommendations.

5 DISCUSSION, CONCLUSIONS and RECOMMENDATIONS

In section 4 the theoretical results are compared to the experimental results. In general the results compare rather well, except for the two-phase correlation where the theoretical results underestimates the experimental results. The mass flow rate for the system operating in single phase is predicted exceptionally well, with the biggest difference between experimental and theoretical mass flow rate being 5.45 %. The comparison of the temperature distribution for single phase operation is reasonable well predicted. The temperature of the primary fluid out of the primary evaporator is predicted with the biggest difference being 4.5 % between the theoretical and experimental temperatures. The temperature in the rest of the primary loop is predicted with the greatest difference being 12 % for operation in single phase flow with a power input of 1 kW. In general the mass flow rate of the primary loop temperature is well predicted within 10 % difference of the experimental mass flow rate and the temperatures are predicted within 12 % difference for single phase operation.

The mass flow rate and temperature distribution of the primary fluid is next compared for 5 kW power inputs that results in the system operating in two-phase mode at steady state. Here it was found that the steady state results and transient response did not compare well with the experimental results. This is due to a couple of factors, one being the use of a single phase heat transfer coefficient, which is not able to predict the heat transfer coefficient. A correlation for the

two-phase heat transfer coefficient will have to be developed that is able to predict the heat transfer coefficient in the primary condenser for two phase flow.

The objectives discussed in Section 1 were achieved; a literature survey was conducted, and presented the current proposed methods for the cooling of the spent/used fuel at a PBMR plant. An experimental setup was built, that was able to simulate the proposed idea in the introduction. From the experimental data it was possible to derive a correlation for the inside pipe heat transfer coefficient of the primary evaporator and for the heat transfer coefficients of the primary condenser. These heat transfer coefficient are only applicable for single phase flow in the loop. The main problem with obtaining a correlation for the two-phase flow heat transfer correlation, is that it is not possible to calculate the Re and Pr numbers from the experimental data, seeing that the vapour content of the liquid in the primary loop cannot be calculated from this data. The heat transfer coefficient was used in the computer algorithm that was adapted from a computer code witted by Dobson in 1988. The results are presented in Chapter 6, in general the computer program predicts the experimental data reasonable well for single phase operation. The computer program will have to be adapted as discussed in the recommendation to properly predict the systems response when operating in two-phase mode.

5.1 Recommendations

5.1.1 Experimental setup
The experimental setup is shown in figures 2 and 3**Error! Reference source not found.** simulated the secondary heat pipe loop by using a continues cooling water system as observed. If this project is continued the secondary heat pipe loop heat the secondary air-cooled condenser has to be designed and incorporated onto the current experimental setup. The current experimental setup was designed and manufactured in such a manner that adding the secondary heat pipe loop will not require redesigning of the current setup.

5.1.2 Heat transfer coefficients
The single phase heat transfer coefficients that where derived in Section 4.4 and 4.5, accurately predict the heat transfer coefficients for single phase operation. However a further study needs to be conducted to develop a correlation that will accurately predict the two-phase flow heat transfer coefficients. This may be achieved by conducting a literature survey on currently available correlations for predicting two-phase flow heat transfer coefficients. And investigate how accurately these correlations predict the heat transfer coefficient.

5.1.3 Computer program:
The QBasic computer program was adapted from a computer program developed by Dobson (1988). The program predicts the experimental results exceptionally well for single phase flow. Improvements can however by made on the primary loop temperature prediction, by incorporating natural convection losses into the code. The program will have to be adapted to incorporate the secondary heat pipe loop if this section is added on to the experimental setup. A major improvement can be made to the computer program by using better two-phase heat transfer coefficients as discussed above.

As mentioned in Chapter 6, the computer program has to be expanded to incorporate the natural convection heat transfer coefficients on the outside of the primary loop, this lead to a more accurate prediction of the measured temperatures.

5.1.4 Scaling:
The scaling of natural circulation loop are a extremely difficult field, normally for the passive cooling of the residual heat in nuclear reactor, a full scale tests are conducted to determine the needed information, such as the heat transfer coefficients, stability, ext. However scaling laws do exist that is used in the prediction of single phase natural circulation systems(Vijayan and Austergesilo, 1994).

Nomenclature
A_x Cross-sectional area, m^2
A_z Longitudinal area of a control area, m^2

A	Area, m^2
a	Speed of sound
B	Any property of the fluid used in the Reynolds transport theorem
C	Velocity of pressure wave in fluid
c_p	Specific heat at constant pressure J/kg.K
c_v	Specific heat at constant volume J/kg.K
D	Diameter, m
E	Energy, J
F	Force, N
Gr_L	Grashof number
g	Gravitational acceleration, 9.81 m/s^2
ID	Inside diameter, m
h	Enthalpy, J/kg.K or Heat transfer coefficient, W/m^{2}K
k	Thermal conductivity, W/m^{2}K
L_c	Characteristic length, m
L	Length, m
$\dot{m}$	Mass flow rate, kg/s
m	Mass, kg
Ma	Mach number
N	Number of tubes
Nu	Nusselt number
OD	Outside diameter, m
P	Pressure, Pa (N/m^2)
Pr	Prandtl number
$\dot{Q}$	Heat transfer, W
R	Thermal resistance, ℃/W or Electrical resistance , ohm
Ra_L	Rayleigh number
Re	Reynolds number
t_{wall}	Wall thickness, m
t	Time, s
T	Temperature, ℃ or K
u	Internal energy per kg, J/kg
u_f	Internal energy for saturated fluid, J/kg
U	Internal energy, J
V	Voltage, V
v	Velocity, m/s
W	Work, J
x	Mass fraction of the fluid
z	Control volume height, m

Greek letters

ρ	Density kg/m^3
β	Coefficient of cubical expansion K^{-1}
σ	Tensile strength, MPa
σ	Stefan-Boltzmann constant, 5.670*10^{-8} W/m^{2}K^4
ϵ	Emissivity
μ	Dynamic viscosity, kg/m.s
α	Void fraction

τ Shear stress, Pa

v Kinematic viscosity, m^2/s

θ Horizontal angle, rad

Subscripts

r Reference

sys System

j   Cooling jacket

i Refers to control volume under consideration

cw Cooling water

com Combined

amb Ambient

avg Average

s Surface

l Liquid

cv Control volume

v Vapour

h Homogeneous

REFERENCES

Budynas, RG and Nisbett, KJ. 2008. *Shigley's Mechanical Engineering Design, eighth edition*. McGraw-Hill.

Cengel, YA. 2006. *Heat and Mass Transfer a Practical Approach,* third edition. McGraw-Hill.

Cengel, YA and Cimbala JM. 2006. *Fluid Mechanics Fundamentals and Applications*. McGraw-Hill.

Cengel, YA and Boles MA. 2007. *Thermodynamics An Engineering Approach Sixth Edition (SI Units)*. McGraw-Hill.

Dobson, RT. 1993. Transient response of a closed loop thermosyphon. *R&D Journal.* **9**(1), pp.32-38.

Dobson, RT. 2010. University of Stellenbosch Personal interview.

Dobson, R.T and Ruppersberg, JC. 2004. A Novel Closed Loop Thermosyphon Heat Pipe Reactor Cavity Cooling System(RCCS) for a Pebble Bed Modular Reactor (PBMR). *In*: *High Temperature reactor technology*. Biejing.

Fuls, WF and MATHEWS, EH. 2006. Passive cooling of the PBMR spent and used fuel tanks. *Nuclear Engineering and design.* **237**, pp.1354-1362.

Fuls, WF and MATHEWS, EH. 2007. Passive cooling of the PBMR spent and used fuel tanks. *Nuclear Engineering and design.* **237**, pp.1354-1362.

IAEA. TECDOC-1474. 2005. *Natural circulation in water cooled nuclear power plants*.

Kroger, DG. 1988. *Air-Heat Exchangers and Cooling Towers*. Department of Mechanical Engineering, University Stellenbosch.

Ruppersberg JC. 2007. *Transient modelling of a loop thermosyphon transient effects in single and two phase natural circulation thermosyphon loops suitable for the reactor cavity cooling of a pebble bed modular reactor*. Department of Mechanical and Mechatronic Engineering University of Stellenbosch.

Verwey, A. 2007. Passive Nuclear Reactor Cooling Using a Loop Thermosyphon. *Final year engineering project.*, University of Stellenbosch

Vijayan, PK and AUSTERGESILO, H. 1994. Scaling laws for single-phase natural circulation loops. *Nuclear Engineering and Design.* **152**, pp.331-347.

Viljoen, C, Fulse, WF & Stoker, P. 2005. The interim fuel storage facility of the PBMR. *Annals of Nuclear Energy.* **32**, pp.1854-1866.

White, FM. 2005. *Fluid Mechanics,* fifth edition. MCGraw-Hill.